

## Local differences in great magnetic storms observed at middle and low latitudes

Qi Li<sup>1</sup>, Yufen Gao<sup>1</sup>, Jianjun Wang<sup>2</sup>, and De-Sheng Han<sup>3</sup>

<sup>1</sup>Institute of Geophysics, China Earthquake Administration, No. 5 Minzuxueyuan Nanlu, Beijing, China

<sup>2</sup>Earthquake Administration of Gansu Province, Lanzhou, China

<sup>3</sup>SOA Key Laboratory for Polar Science, Polar Research Institute of China, Shanghai, China

(Received January 15, 2009; Revised May 9, 2009; Accepted May 9, 2009; Online published October 19, 2009)

The dependence of the storm-time amplitude on longitude and latitude was analyzed by statistically investigating great magnetic storms observed at different observatories. First, we compared the storm-time ranges observed at Beijing Observatory (BJI) and San Juan Observatory (SJG) to reveal their longitudinal dependence. It was found that the difference between BJI and SJG could be fitted by the 4-order Fourier series approximation, and the storm-time  $H$  ranges at dawn were less than those at dusk. Second, we carried out a case study of two typical storms, and analyzed the focused local time when peak storm-time  $H$  ranges occurred. The results confirmed the above conclusion. Third, a statistical study was conducted for all magnetic storms observed at the 120°E magnetic chain in eastern China for 1995–2004 to reveal the latitudinal dependence of storm-time ranges. It was found the relationship depended on the activity of analyzed storms and became complicated for giant storms with  $D_{st} \leq -300$  nT.

**Key words:** Local differences in great storms, storm-time range, local time, latitude dependence.

### 1. Introduction

A magnetic storm is a global geomagnetic field disturbance characterized by a distinct decrease in the horizontal ( $H$ ) component of the magnetic field at mid and low latitudes. It is generally accepted that the source of the magnetic disturbance is a ring current circling the Earth in the equatorial plane. The strength of a magnetic storm is usually measured by the  $D_{st}$  index, which is derived from hourly values of the  $H$  component of the geomagnetic field recorded at four low-latitude stations. The derivation of the  $D_{st}$  index is based on the assumption that the geomagnetic variation caused by the ring current is axially symmetrical and has no longitudinal/local time dependence. Therefore the  $D_{st}$  index reflects the  $H$  variation caused by the symmetrical ring current. However, the  $H$  magnetic perturbations recorded by mid-latitude stations during the main phase of a storm are obviously asymmetric in longitude (Chapman and Bartels, 1940), and the  $H$  amplitude is related to the local time. The current systems responsible for magnetic storms include the partial ring current, field-aligned current, magnetopause current, and tail current as well as the ring current. As a result, the  $D_{st}$  derivation does not only reflect the geomagnetic field variations on the ground caused by the symmetrical ring current, but also includes those variations caused by other above-mentioned currents. Liemohn *et al.* (2001) pointed out that the partial ring current plays a dominant role in producing the stormtime  $D_{st}^*$ . Turner and Baker (2000) and Ohtani *et al.* (2001) found that the contribution

of the tail current to  $D_{st}$  is approximately 25%.

There has been much research on the asymmetric development of storms (Akasofu and Chapman, 1964; Kamide and Fukushima, 1971; Crooker and Siscoe, 1974, 1981; Kamide and Matsusita, 1979; Clauer and McPherron, 1980; Sun *et al.*, 1984; Xu, 1992; Iyemori, 2000; Maltsev, 2004). Most research has investigated a possible cause of the asymmetric development by studying different current systems and storms. Grafe (1999) suggested that only the partial ring current, and no symmetric ring current, exists. Kawasaki and Akasofu (1971) proposed the ASYM index to measure the asymmetric development of magnetic storms, which is similar to the ASY index published monthly by Kyoto University.

Space weather forecasting is carried out all around the world, and forecasting geomagnetic field disturbances is an important part of that effort. It is well known that magnetic storms harm space-based technical systems such as satellite communication and navigation systems. Actually, ground-based technical systems such as those used in directional drilling, electricity networks and underground pipelines are also affected by magnetic storms. For ground-based technical systems, local disturbances in the magnetic field are more important than globally averaged activity level. Therefore, studying local differences in magnetic storms is a worthwhile endeavor.

Most of the research work on the regional disturbances of the geomagnetic field has focused on its theoretical model (Fukushima and Kamide, 1973; Takahashi *et al.*, 1991; Jordanova *et al.*, 2003). There have not been many statistical studies on this subject. Iyemori (1990) derived the longitudinally symmetric and asymmetric components of  $H$

Table 1. Ground observatories from which data are used in this paper.

Station name	Code	Geographic (°)		Geomagnetic (°)	
		longitude	latitude	longitude	latitude
San Juan	SJG	293.88	18.38	5.47	29.04
Manzhouli	MZL	117.4	49.6	192.50	39.25
Beijing	BJI	116.18	40.06	186.66	29.44
Wuhan	WHN	114.6	30.5	190.66	20.10
Qiongzong	QGZ	109.8	19.0	186.31	8.54

and east-west ( $D$ ) using data from 10 mid-latitude stations. Grafe *et al.* (1996) investigated the temporal evolution of the low-latitude disturbance field at different magnetic local times for several storms of different activity. In this paper, we attempt to reveal the dependence of the main phase ranges of great magnetic storms on longitude and latitude. The storm-time amplitudes at Beijing Observatory (BJI) and San Juan Observatory (SJG) are compared to reveal the difference between dawn and dusk and that between noon and midnight sectors. All magnetic storms for 1995–2004 are investigated to reveal the dependence of the storm-time  $H$  and  $D$  amplitudes on latitude.

## 2. Data Preparation

The geomagnetic field disturbance recorded by a ground station depends on its location relative to the sun. For those stations located at the same latitude, the dependence of the recorded storm-time amplitude on longitude is that on local time. Therefore, it is important to choose stations located approximately at the same latitude to study the dependence of the storm-time  $H$  and  $D$  amplitudes on longitude. Fortunately, BJI and SJG make an ideal pair of observation stations in that they are approximately located not only on the same geomagnetic longitude circle but also the same geomagnetic latitude circle. The differences between the geomagnetic local times of BJI and SJG and their local times are less than one hour, so the local time is used in this paper. The averaged  $S_q$  pattern on five quiet days was subtracted from the hourly  $H$  amplitude and the result divided by  $\cos \theta$  to correct for the magnetic equator, where  $\theta$  is the geomagnetic latitude at each observatory. In Section 3.1, the residual data after subtraction of  $S_q$  were rotated by the angle between the direction of the geomagnetic dipole field and the direction of the horizontal vector at the observatory to avoid mixing the effect of the ring current with that of the  $D$  component.

To determine the dependence of the storm-time  $H$  and  $D$  amplitudes on latitude, the data recorded by the chain of magnetic observatories in eastern China were used. The chain comprises four observatories; from north to south, Manzhouli Observatory (MZL), BJI, Wuhan Observatory (WHN) and Qiongzong (QGZ). The four observatories are located approximately in the same longitude circle, and the latitude difference between two neighboring observatories is about  $10^\circ$ .  $S_q$  was also subtracted from  $H$  and  $D$  hourly data before the main phase range and the disturbance range were calculated.

Information for the above-mentioned ground observatories is given in Table 1.

## 3. Dependence of the Storm-time $H$ and $D$ Amplitudes on Longitude

### 3.1 Local differences in the storm-time amplitude between BJI and SJG

To analyze the differences in the storm-time amplitude between BJI and SJG, 21 storms with  $D_{st} < -100$  nT for 1998–2000 were selected. Table 2 gives parameters for the 21 storms including the occurrence date, the peak value of the  $D_{st}$  index and corresponding Beijing Local Time (BLT = UT + 8), and the hourly averaged  $D$  and  $H$  components for BJI and SJG at the same time as well as the difference between them.

Table 2 shows the difference  $\Delta H$  between the  $H$  component for BJI and that for SJG (the value for BJI minus the value for SJG) fluctuated greatly, and was not related to the  $D_{st}$  index. Some  $\Delta H$  values were close to or even larger than the corresponding  $D_{st}$  index. Most  $D$  values in Table 2 were negative; that is, the magnetic declination was westwards from the geographical north when the studied storms were deeply developed.

Figure 1 shows the dependence of  $\Delta H$  on BLT. The black squares are observed values given in Table 2, and show an obvious dependence on local time. It is obvious that  $\Delta H$  was positive before noon and negative after, which means that the magnetic field was more active at dusk than it was at dawn. The curve in Fig. 1 is the result of 4-order Fourier series approximation, and the fitting formula is

$$\begin{aligned}
 Y = & -21.66 + 108.04 \sin\left(\frac{\pi x}{12}\right) + 8.32 \cos\left(\frac{\pi x}{12}\right) \\
 & -24.27 \sin\left(\frac{2\pi x}{12}\right) - 1.07 \cos\left(\frac{2\pi x}{12}\right) \\
 & + 12.1 \sin\left(\frac{3\pi x}{12}\right) + 7.4 \cos\left(\frac{3\pi x}{12}\right) \\
 & -6.48 \sin\left(\frac{4\pi x}{12}\right) - 10.19 \cos\left(\frac{4\pi x}{12}\right)
 \end{aligned}$$

Here  $Y$  is the value  $\Delta H$  and  $x$  is the BLT.

From above formula, the minimum of  $Y$  was  $-126.98$  nT at 17.48 BLT and the maximum was  $99.78$  nT at 08:36 BLT. The values indicate the peak differences between BJI and SJG were at dawn and dusk, respectively, and the average absolute value  $113.38$  nT was the intensity of a great magnetic storm.  $\Delta H$  was close to zero at noon and midnight. It is obvious that the curve in Fig. 1 was not axially symmetrical around the line  $y = 0$ , but the line  $y = -13.6$  nT. As a result, the peak value of  $\Delta H$  at dusk was more than that at dawn. Li *et al.* (2005) found a similar result comparing the BJI data and the  $D_{st}$  index. A possible

Table 2. Parameters for the 21 selected great storms with  $D_{st} \leq -100$  nT for 1998–2000.

DD/mm/yy	$D_{st}$	BLT	Bji_D/nT	Sjg_D/nT	Bji_H/nT	Sjg_H/nT	$\Delta D$ (BJI–SJG)/nT	$\Delta H$ (BJI–SJG)/nT
11/02/00	–133	19	–10	–36	–189	–79	26	–110
23/05/00	–147	16	–40	–18	–165	–89	–21	–76
15/07/00	–301	8	–15	–70	–248	–312	55	65
11/08/00	–235	17	–50	–64	–262	–104	14	–157
17/09/00	–201	7	–44	–17	–149	–261	–27	113
12/10/00	–107	22	–5	–15	–119	–67	9	–52
28/10/00	–127	11	–20	–16	–107	–109	–4	2
06/11/00	–159	5	–37	–20	–125	–180	–16	55
13/01/99	–112	4	–11	–19	–80	–131	8	52
18/02/99	–123	1	–21	–18	–105	–100	–3	–5
22/09/99	–173	7	–60	–41	–122	–211	–20	89
21/10/99	–237	14	–59	–18	–256	–171	–42	–85
10/03/98	–116	4	–26	–27	–55	–140	2	84
03/05/98	–205	13	–122	39	–233	–96	–161	–136
25/06/98	–101	12	–7	–2	–92	–92	–4	0
06/08/98	–138	19	–29	–51	–171	–56	22	–115
26/08/98	–155	17	–18	–49	–194	–59	30	–135
18/10/98	–112	23	0	7	–134	–101	–7	–33
07/11/98	–149	14	–2	–77	–190	–35	75	–155
09/11/98	–142	1	19	–17	–126	–138	37	13
13/11/98	–131	5	–2	–32	–99	–132	31	33

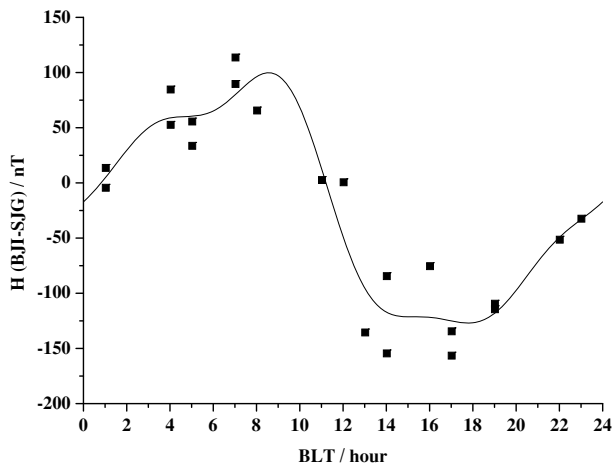


Fig. 1. Dependence of  $\Delta H$  (value for BJI minus value for SJG) on BLT for 21 great storms in 1998–2000. Black squares indicate observed values and the curve indicates the result of 4-order Fourier series approximation.

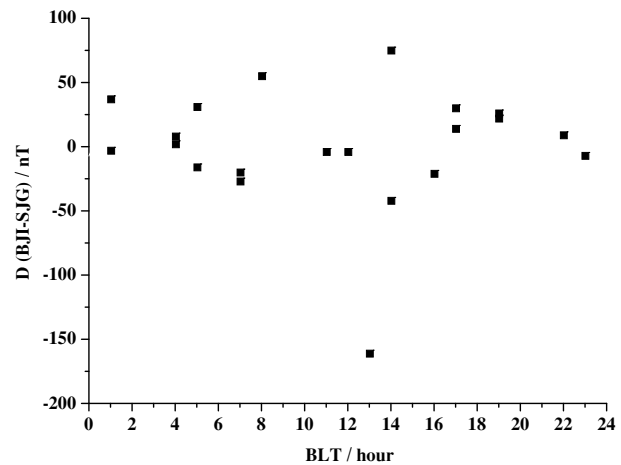


Fig. 2. Dependence of  $\Delta D$  (value for BJI minus value for SJG) on BLT for 21 great storms in 1998–2000. Black squares indicate observed values.

reason could be that the partial ring current covers about 2/3 of the ring current.

Figure 2 shows the difference  $\Delta D$  between the peak  $D$  amplitude for BJI and that for SJG (the value for BJI minus the value for SJG), but no clear regulation was found.

### 3.2 Case study for two typical magnetic storms recorded by BJI and SJG

Sometimes, a single magnetic storm shows a clearer difference between dawn and dusk. Figure 3 shows the  $D_{st}$  index and  $H$  variation for BJI and SJG during two typical magnetic storms. Figure 3(a) shows the magnetic storm of August 26–28, 1998. The peak value of the  $D_{st}$  index was  $-155$  nT at 17:00 BLT when it was dusk at BJI and dawn at SJG. At that moment, the  $H$  value for BJI and SJG

was  $-222$  nT and  $-66$  nT, respectively. The difference was 156 nT. It should be noted that the peak  $H$  value  $-225.5$  nT for BJI did not appear at the same time as the peak  $D_{st}$  value did, but one hour earlier. Furthermore, the  $H$  amplitude for SJG suddenly changed from descending to ascending, and reached a peak value of  $-22.7$  nT while the  $H$  amplitude for BJI reached its minimum value. The difference between them was 202.8 nT. Such a distinct difference appearing at dawn and dusk deserves to be noted. Figure 3(b) shows the magnetic storm of June 25–27, 1998. The peak value of the  $D_{st}$  index was  $-101$  nT at 12:00 BLT, which was noon for BJI and midnight for SJG. The  $H$  amplitudes for both BJI and SJG at that moment were  $-105.3$  nT. The dependence of the  $H$  amplitude on local time during both magnetic storms was as seen in Fig. 1.

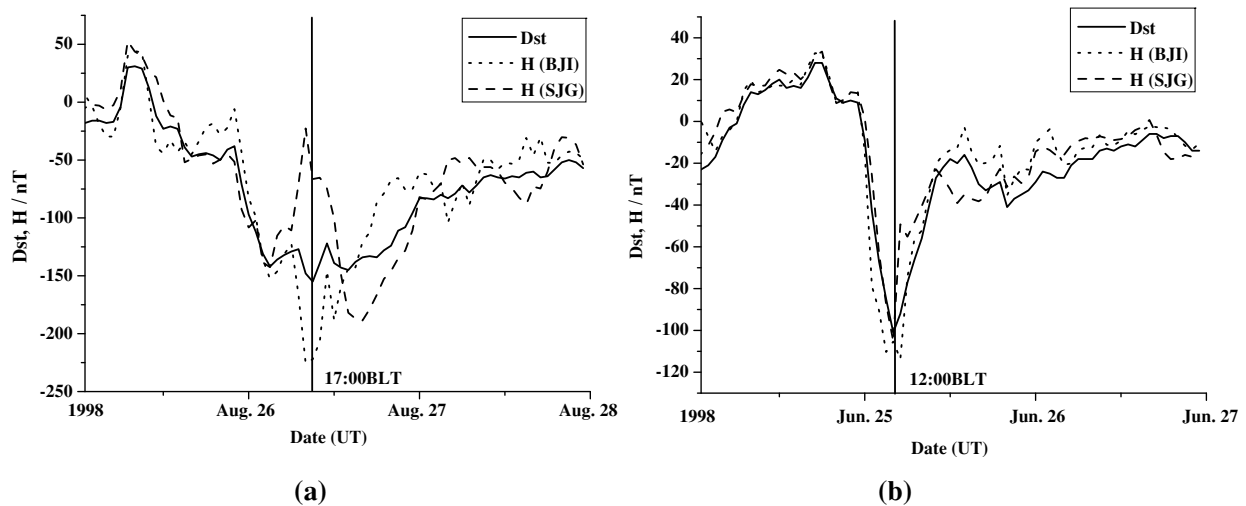


Fig. 3.  $D_{st}$  index and the  $H$  amplitude curve for BJI and SJG during two typical magnetic storms.

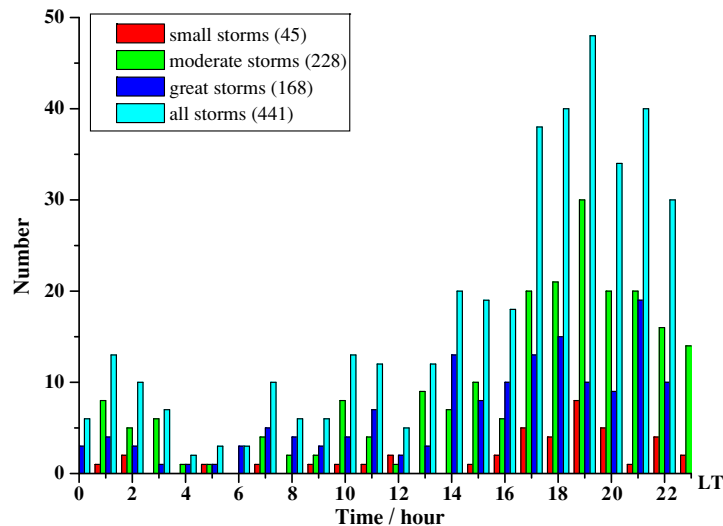


Fig. 4. Number of peak  $H$  values occurring at each local time sorted by the activity of storms. The values in parentheses are the storm numbers of each storm category.

### 3.3 Favored time for the peak storm-time $H$ amplitude at BJI

The above results show that the peak  $H$  amplitude was usually larger at dusk than at dawn during storms. Therefore, it can be concluded that most peak storm-time  $H$  amplitudes appear at dusk for an observatory. We classified all the magnetic storms reported by BJI for 1979–1999 into three categories following the method of Gonzalez *et al.* (1994); that is,  $D_{st} \leq -100$  nT indicates a great or intense magnetic storm,  $-50$  nT  $\geq D_{st} > -100$  nT indicates a moderate storm and  $-30$  nT  $\geq D_{st} > -50$  nT indicates a weak storm. The number of peak  $H$  amplitudes for each local time is shown in Fig. 4 sorted by the activity of storms. Figure 4 shows that most peak  $H$  amplitudes occurred at dusk for all categories of storms, which is in accordance with the conclusion reached in Sections 3.1 and 3.2.

### 4. Dependence of the Storm-time $H$ and $D$ Amplitudes on Latitude

The main phase range of the  $H$  component (the difference between the hourly value just before the beginning of storms and the minimum hourly value of the main phase) and the disturbance range of the  $D$  component (the difference between the maximum and minimum hourly values of a storm-time magnetic field) recorded by the magnetic chain in eastern China for 1995–2004 were calculated and sorted by the activity of the storms. Tables 3 and 4 show the dependence of the main phase range of the  $H$  component and the disturbance range of the  $D$  component for each observatory, respectively. The values in parentheses in Tables 3 and 4 are the number of storms in each storm category recorded at BJI and the upper and lower boundaries of the  $D_{st}$  index for the category. The number of storms with  $D_{st} \leq -100$  nT recorded by other observatories was the same as the number recorded by BJI. The number of moderate storms and small storms recorded by other observatories differed at most by two storms with the number recorded

Table 3. Main phase range of the  $H$  component (unit is nT) derived using data from four observatories during 1995–2004. The first values in the parentheses are the numbers of storms in each category of storm recorded by BJI and the second and the third values are the upper and lower boundaries of the  $D_{st}$  index for the category.

Code	All storms (128)	Giant storms (1, $-400, -500$ )	Intense storms (5, $-300, -400$ )	Intense storms (10, $-200, -300$ )	Great storms (69, $\leq -100$ )	Moderate storms (49, $-50, -100$ )	Small storms (10, $-30, -50$ )
MZL	128.96	525.6	343.2	235.14	166.56	87.53	72.56
BJI	136.30	465	330.4	235.76	173.21	95.39	82.04
WHN	141.52	471.94	331.616	244.834	179.64	100.10	81.44
QGZ	153.46	509.6	360.04	270.68	194.85	108.30	89.16

Table 4. Disturbance range of the  $D$  component (unit is nT) derived using data from four observatories during 1995–2004. The first values in the parentheses are the numbers of storms in each storm category recorded by BJI and the second and third values are the upper and lower boundaries of the  $D_{st}$  index for the category.

Code	All storms (128)	Giant storms (1, $-400, -500$ )	Intense storms (5, $-300, -400$ )	Intense storms (10, $-200, -300$ )	Great storms (69, $\leq -100$ )	Moderate storms (49, $-50, -100$ )	Small storms (10, $-30, -50$ )
MZL	93.42	184.58	193.30	156.00	115.28	71.06	52.21
BJI	69.63	135.32	151.83	122.53	85.61	53.24	39.70
WHN	52.70	89.53	111.35	93.22	63.72	41.56	31.30
QGZ	43.59	93.79	96.97	71.13	52.17	34.91	26.87

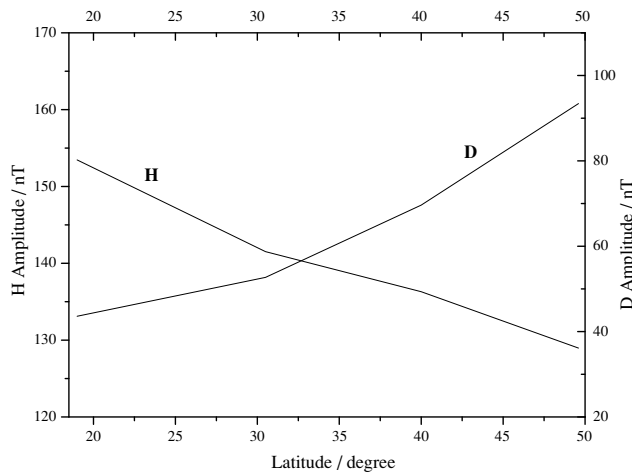


Fig. 5. Dependence of the main phase range of the  $H$  component and the disturbance range of the  $D$  component on latitude for all storms.

by BJI, and this did not affect the comparison among different observatories. There was only one giant storm with  $-400 \text{ nT} \geq D_{st} > -500 \text{ nT}$  for 1995–2004, which occurred on November 20, 2003, and its peak  $D_{st}$  was  $-422$ .

Table 3 shows the averaged  $H$  main phase range of all storms and storms with  $D_{st} > -300 \text{ nT}$  almost linearly increased with decreasing latitude. The dependence of the averaged main phase range of the  $H$  component on latitude for all storms is shown in Fig. 5. Table 3 shows that the above regulation was not suitable for intense storms with  $D_{st} \leq -300$ . For storms with  $-400 < D_{st} \leq -300$ , the averaged  $H$  main phase range for MZL was larger than ranges for BJI and WHN, but was less than that for QGZ. However, for storms with  $-400 \text{ nT} \geq D_{st} > -500 \text{ nT}$ , the averaged  $H$  main phase range for MZL was at least 16 nT larger than that for any other studied observatory.

Table 4 shows the averaged  $D$  disturbance range for all categories of storms almost had the same dependence on latitude (except for the giant storm of November 20, 2003);

that is, the averaged  $D$  disturbance range decreased as the latitude decreased. The dependence of the averaged disturbance range of the  $D$  component for all storms on latitude is also shown in Fig. 5.

Figure 6 shows the dependence of the main phase range of the  $H$  component and the disturbance range of the  $D$  component on latitude for all storms on different local time sectors where the peak storm-time  $H$  amplitude appeared. The same scale is used in Fig. 5 and Fig. 6. It is found that Fig. 6(a) and (c) is similar with Fig. 5. However, the difference between the  $H$  main phase range of QGZ and MZL is larger in Fig. 6(b) and smaller in Fig. 6(d) than that in Fig. 5.

The averaged  $D$  disturbance range decreased as the latitude decreased at different local time sectors as Fig. 6 shows.

## 5. Conclusion and Discussion

The dependence of magnetic storms on local time and latitude is analyzed in this paper. Statistical analysis for 21 great storms with  $D_{st} \leq -100 \text{ nT}$  from 1998 to 2000 shows that the storm-time  $H$  amplitude was obviously different between BJI and SJG. The result of 4-order Fourier series approximation shows that the storm-time  $H$  amplitude was larger at dusk than at dawn, and was almost equal to the average value at noon and midnight. The difference between the storm-time  $H$  amplitudes at dusk and at dawn was more than 100 nT, and reached the intensity of a great magnetic storm.

Statistical analysis shows that most peak  $H$  amplitudes occurred at dusk for all categories of storms, which is consistent with the conclusion achieved in Sections 3.1 and 3.2. This indicates that the magnetic field disturbance during magnetic storms is not only related to the symmetrical ring current, but also to other current systems such as the asymmetric ring current and ionospheric current.

The analysis of data recorded by the chain of magnetic observatories in eastern China shows that the averaged  $H$

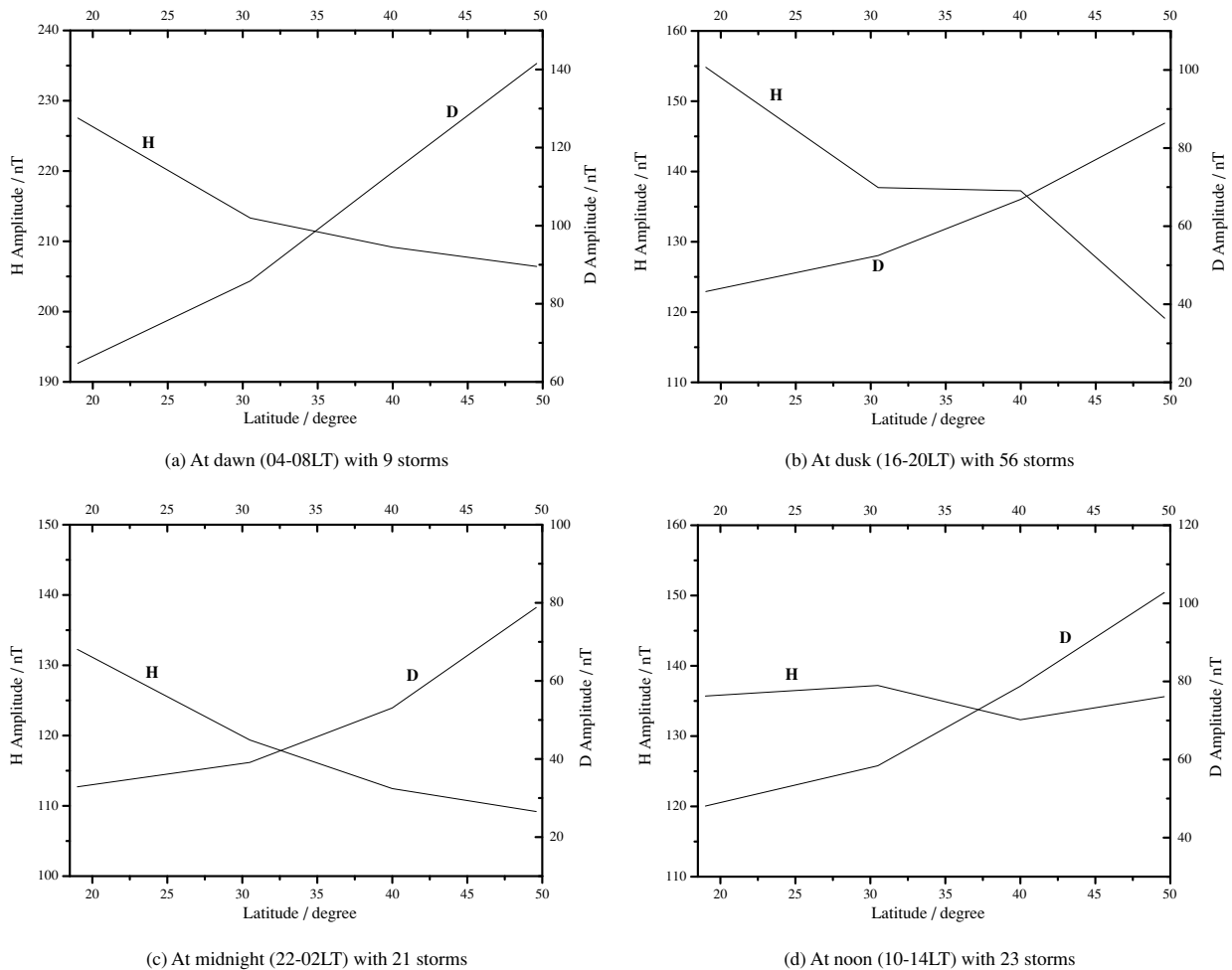


Fig. 6. Dependence of the main phase range of the  $H$  component and the disturbance range of the  $D$  component on latitude for all storms on different local time sectors where the peak storm-time  $H$  amplitude appears.

main phase range of storms with  $D_{st} > -300$  linearly increased as the latitude decreased, which agrees with the common knowledge that storm-time magnetic field variation is caused by equatorial ring current, especially during the main phase of storms. However, the result derived from storms with  $D_{st} \leq -300$  nT differs. For example, the main phase range of the  $H$  component was largest at the northernmost observatory MZL and not at QGZ, which is nearest the equator, during the giant storm of November 11, 2003. This cannot be explained by the ring current, and current systems in both the magnetosphere and ionosphere could be very complicated during such giant storms. Feldstein *et al.* (1997) pointed out that the center of an auroral electrojet lowers when the magnetic field is active, and it could lower almost  $10^\circ$  in latitude during great storms. Therefore, measurements by observatories at upper mid-latitudes could also be affected by auroral electrojets. It is also possible that the plane of the ring current tilts during strong storms so that the storm-time range is larger at observatories at upper mid-latitudes.

Figure 6 shows that the  $H$  main phase range increased as the latitude decreased at different local time sectors on average especially at dawn and midnight as shown in Fig. 6(a) and Fig. 6(c), which may suggest that the ring current still plays the main role during the main phase of geomagnetic

storms. The difference between the  $H$  main phase range of QGZ and MZL is larger in Fig. 6(b) than those in other time sectors, which could be affected by the partial ring current at dusk. However, the difference between the  $H$  main phase range of WHN and BJI is very small in Fig. 6(b). BJI is located in an underground magnetic anomaly area, which may be the reason for that. The result shown by Fig. 6(d), the  $H$  main phase range at noon only changes a little as the latitude increased, suggest that ionospheric currents are contaminated in the latitude distribution of  $H$  component although  $S_q$  has been removed. WHN is located near the center of  $S_q$ , so the  $H$  amplitude recorded by WHN is only a little affected by ionospheric currents. On the other hand, the recorded  $H$  amplitude decreased in QGZ but increased in MZL and BJI affected by ionospheric currents. So the influence on the  $H$  main phase range from ionospheric currents cannot be neglected at noon.

The averaged  $D$  disturbance range decreased as the latitude decreased for most categories of storms. As we know, the  $D$  component is mainly affected by field-aligned current, so a possible reason for the above result is that the field-aligned current has a stronger effect on the magnetic field at higher latitude.

In general, the local activity of the magnetic field differs from one area to another, and the difference could be larger

than 100 nT. The British Geological Survey indicated that the required precision of magnetic field data for oil directional drilling is  $F < 50$  nT and  $D < 6$ . Industries such as electricity networks and underground pipelines also rely on information of local magnetic field disturbances, but the present global space weather forecast cannot satisfy their requirements. The dependence of technical systems on local magnetic disturbances will become stronger as science and technology develop. Therefore, the local difference cannot be neglected, and a local magnetic field forecast based on the global space weather forecast would be useful in the near future.

**Acknowledgments.** This research was supported by the project Environment Building for S&T Industries (2005DKA64000). The data of magnetic storms and the data recorded by observatories in China were provided by the Geomagnetic Network of China, Institute of Geophysics, China Earthquake Administration. The  $D_{st}$  index and data from San Juan Observatory were downloaded from the website <http://swdcd.db.kugi.kyoto-u.ac.jp/>. The results presented in this paper rely on the data collected at San Juan Geomagnetic Observatory. We thank USGS Geomagnetism Program, for supporting its operation and INTERMAGNET for promoting high standards of magnetic observatory practice ([www.intermagnet.org](http://www.intermagnet.org)). Also, the authors would like to thank both reviewers for their helpful advice.

## References

- Akasofu, S.-I. and S. Chapman, On the asymmetric development of magnetic storm fields in low and middle latitudes, *Planet. Space Sci.*, **12**, 607–626, 1964.
- Chapman, S. and J. Bartels, *Geomagnetism*, 274 pp., Clarendon Press, Oxford, 1940.
- Clauer, C. R. and R. L. McPherron, The relative importance of the interplanetary electric field and magnetosphere substorms on partial ring current development, *J. Geophys. Res.*, **85**(A12), 6747–6759, 1980.
- Crooker, N. U. and G. L. Siscoe, Model geomagnetic disturbance from asymmetric ring currents particles, *J. Geophys. Res.*, **79**, 589–594, 1974.
- Crooker, N. U. and G. L. Siscoe, Birkeland current as the cause of the low-latitude asymmetric disturbance field, *J. Geophys. Res.*, **86**(A13), 11201–11210, 1981.
- Feldstein, Y. I., A. Grafe, L. I. Gromova, and V. A. Popov, Auroral electrojets during geomagnetic storms, *J. Geophys. Res.*, **102**(A7), 14223–14235, 1997.
- Fukushima, N. and Y. Kamide, Partial ring current models for worldwide geomagnetic disturbances, *Rev. Geophys. Space Phys.*, **11**(4), 795–853, 1973.
- Gonzalez, W. D., J. A. Joselyn, Y. K. Kamide, H. W. Kroehl, G. Rostoker, B. T. Tsurutani, and V. M. Vasyliunas, What is a geomagnetic storm?, *J. Geophys. Res.*, **99**(A4), 5771–5792, 1994.
- Grafe, A., Are our ideas about Dst correct?, *Ann. Geophys.*, **17**, 1–10, 1999.
- Grafe, A. *et al.*, Evolution of the low-latitude geomagnetic storm field and the importance of turbulent diffusion for ring current particle losses, *J. Geophys. Res.*, **101**(A11), 24,689–24,706, 1996.
- Iyemori, T., Storm-time magnetospheric currents inferred from mid-latitude geomagnetic field variations, *J. Geomag. Geoelectr.*, **42**, 1249–1265, 1990.
- Iyemori, T., Formation of the storm-time ring current and the Dst field: some recent topics, in *magnetospheric current systems*, Geophysical Monograph 118, 331–338, 2000.
- Jordanova, V. K. *et al.*, Ring current asymmetry from global simulations using a high-resolution electric field model, *J. Geophys. Res.*, **108**(A12), 1443, 2003.
- Kamide, Y. and N. Fukushima, Analysis of magnetic storms with Dr-indices for equatorial ring current field, *Rep. Ionos. Space Res. Jpn.*, **25**, 125–162, 1971.
- Kamide, Y. and S. Matsusita, Simulation studies of ionospheric electric fields and currents in relation to field-aligned currents (2. substorms), *J. Geophys. Res.*, **84**(A8), 4099–4115, 1979.
- Kawasaki, K. and S. I. Akasofu, Low-latitude DS component of geomagnetic storm field, *J. Geophys. Res.*, **76**, 2396–2405, 1971.
- Li, Q., Y. Gao, and D. Han, Analysis on magnetic storms reported by Beijing observatory, *J. Atmos. Sol.-Terr. Phys.*, **67**(10), 853–861, 2005.
- Liemohn, M. W. *et al.*, Dominant role of the asymmetric ring current in producing the stormtime Dst\*, *J. Geophys. Res.*, **106**(A6), 10,883–10,904, 2001.
- Maltsev, Y. P., Points of controversy in the study of magnetic storms, *Space Sci. Rev.*, **110**, 227–267, 2004.
- Ohtani, S. *et al.*, Storm-substorm relationship: Contribution of the tail current to Dst, *J. Geophys. Res.*, **106**(A10), 21,199–21,209, 2001.
- Sun, W., B.-H. Ahn, and S.-I. Akasofu, A comparison of observed mid-latitude magnetic disturbance fields with those reproduced from the high-latitude modeling current system, *J. Geophys. Res.*, **89**(A12), 10881–10889, 1984.
- Takahashi, S., M. Takeda, and Y. Yamada, Simulation of storm-time partial ring current system and the dawn-dusk asymmetry of geomagnetic variation, *Planet. Space Sci.*, **39**, 821–832, 1991.
- Turner, N. E. and D. N. Baker, Evaluation of the tail current contribution to Dst, *J. Geophys. Res.*, **105**(A3), 5431–5439, 2000.
- Xu, W. Y., Geomagnetic effects of the inner magnetospheric current system, *Chin. J. Geophys.*, **35**(1), 1–8, 1992.

Q. Li (e-mail: darcyli@163.com), Y. Gao, J. Wang, and D.-S. Han